E3 and M2 transition strengths in $^{209}_{83}$Bi

O.J. Roberts,[1,2] C.R. Niţă,[1,3] A.M. Bruce,[1] N. Mărginean,[3] D. Bucurescu,[3] D. Deleanu,[3] D. Filipescu,[3] N.M. Florea,[3,4] I. Gheorghe,[3,5] D. Ghiţă,[3] T. Glodariu,[3] R. Lica,[3] R. Mărginean,[3] C. Mihai,[3] A. Negret,[3] T. Sava,[3] L. Stroe,[3] R. Şuvăilă,[3] S. Toma,[3] T. Alharbi,[6,7] T. Alexander,[6] S. Aydin,[8] B.A. Brown,[9] F. Browne,[1] R.J. Carroll,[6] K. Mulholland,[10] Zs. Podolyák,[6] P.H. Regan,[6,11] J.F. Smith,[10] M. Smolen,[10] and C.M. Townsley[6]

[1] *School of Computing, Engineering and Mathematics, University of Brighton, Brighton BN2 4GJ, UK*
[2] *School of Physics, University College Dublin, Belfield, Dublin 4, Ireland*
[3] *Horia Hulubei National Institute of Physics and Nuclear Engineering, P.O.BOX MG-6, Bucharest-Magurele, Romania*
[4] *University Politehnica of Bucharest, 011061, Bucharest, Romania*
[5] *Faculty of Physics, University of Bucharest, RO-077125, Bucharest, Romania*
[6] *Department of Physics, University of Surrey, Guildford GU2 7XH, UK*
[7] *Department of Physics, Almajmaah University, P.O. Box 66, 11952, Saudi Arabia*
[8] *Department of Physics, University of Aksaray, Aksaray, Turkey*
[9] *Department of Physics and Astronomy, and National Superconducting Cyclotron Laboratory, Michigan State University, East Lansing, Michigan 48824-1321, USA*
[10] *Nuclear Physics Research Group, The University of the West of Scotland, Paisley PA1 2BE, UK*
[11] *National Physics Laboratory, Teddington TW11 0LW, UK*

(Dated: October 22, 2015)

The $1i_{\frac{13}{2}} \rightarrow 1h_{\frac{9}{2}}$ ($M2$) and $3s_{\frac{1}{2}} \rightarrow 2f_{\frac{7}{2}}$ ($E3$) reduced proton transition probabilities in $^{209}_{83}$Bi have been determined from the direct half-life measurements of the $\frac{13}{2}^+_1$ and $\frac{1}{2}^+_1$ states using the ROmanian array for γ-ray SPectroscopy in HEavy ion REactions (*ROSPHERE*). The $\frac{13}{2}^+_1$ and $\frac{1}{2}^+_1$ states were found to have $T_{\frac{1}{2}}$=0.120(15) ns and $T_{\frac{1}{2}}$=9.02(24) ns respectively. Angular distribution measurements were used to determine an $E3/M2$ mixing ratio of δ=-0.18(2) for the 1609 keV γ-ray transition de-exciting the $\frac{13}{2}^+_1$ state. This value for δ was combined with the measured half-life to give reduced transition probabilities of B($E3, \frac{13}{2}^+_1 \rightarrow \frac{9}{2}^-_1$)=13(2)$\times 10^3$ e^{2}fm^6 and B($M2, \frac{13}{2}^+_1 \rightarrow \frac{9}{2}^-_1$)=0.038(5)$\times 10^3$ μ_N^2 fm^2. These values are in good agreement with calculations within the finite Fermi system. **The extracted value of B($E3, \frac{1}{2}^+_1 \rightarrow \frac{7}{2}^-_1$)=6.3(2)$\times 10^3$ e^{2}fm^6 can be explained by a small ($\sim$6%) admixture in the wavefunction of the $\frac{1}{2}^+_1$ state.**

PACS numbers: 21.10.Tg, 23.20.En, 23.20.Gq, 23.20.Js, 23.20.Lv, 25.70.Hi, 27.80.+W, 29.30.Kv, 29.40.Mc

I. INTRODUCTION

The ground state of $^{209}_{83}$Bi can be described as a single $1h_{\frac{9}{2}}$ proton coupled to the $^{208}_{82}$Pb core [1]. **A septuplet of levels with spins between $\frac{3}{2}$ and $\frac{15}{2}$, formed due to the coupling of the same proton to the 3^- octupole vibrational state in of the $^{208}_{82}$Pb core, is observed at an excitation energy of $\sim$2.6 MeV. The three states below this septuplet are predominately formed from the excitation of the single proton [1].** Present information on the properties of low-lying states in $^{209}_{83}$Bi was determined from **comprehensive inelastic scattering [2–6]**, Coulomb excitation [7–11], direct decay time [12–14] and multi-nucleon transfer reaction [1, 15] measurements.

In cases where the properties of low-lying excitations in single-nucleon systems are simple to interpret and can be described using basic theoretical models, effective multipole operators have been shown to describe static electric and magnetic multipole moments and low-energy-transition rates [16]. Re-normalisation effects are incorporated in the effective multipole operators, which in the case of electric multipoles, mainly arise from the core polarisation mechanism [17]. Because the uncertainties for configuration mixing in the lead region are smaller than in other regions around closed-shell nuclei (e.g. ^{16}O,^{40}Ca), Mottelson has advocated that the lead region is possibly the best place to explore the effective charge phenomena [18]. Therefore, this article presents new measurements on low-lying levels in $^{209}_{83}$Bi from which the strength of the single-particle $1i_{\frac{13}{2}} \rightarrow 1h_{\frac{9}{2}}$ and $3s_{\frac{1}{2}} \rightarrow 2f_{\frac{7}{2}}$ transitions have been extracted.

The strength of the $1i_{\frac{13}{2}} \rightarrow 1h_{\frac{9}{2}}$ $M2$ transition can be obtained from the half-life of the $\frac{13}{2}^+_1$ level and the $E3/M2$ mixing ratio of the depopulating transition. The latter is required because the $\frac{13}{2}^+_1$ state (E$_x$=1609 keV) is known to be a mixture of a single proton in the $1i_{\frac{13}{2}}$ shell coupled to the 0^+ ground state in the $^{208}_{82}$Pb core, and a single proton in the $1h_{\frac{9}{2}}$ shell coupled to the 3^- octupole vibrational state in $^{208}_{82}$Pb [7, 19, 20], as shown schematically in Fig. 1.

The B($E3$) excitation probability to the $\frac{13}{2}^+_1$ level has been measured in Coulomb excitation experiments using α and ^{16}O beams to be 12.4(32)$\times 10^3$ e^{2}fm^6 [7] and 22(8)$\times 10^3$ e^{2}fm^6 [8]

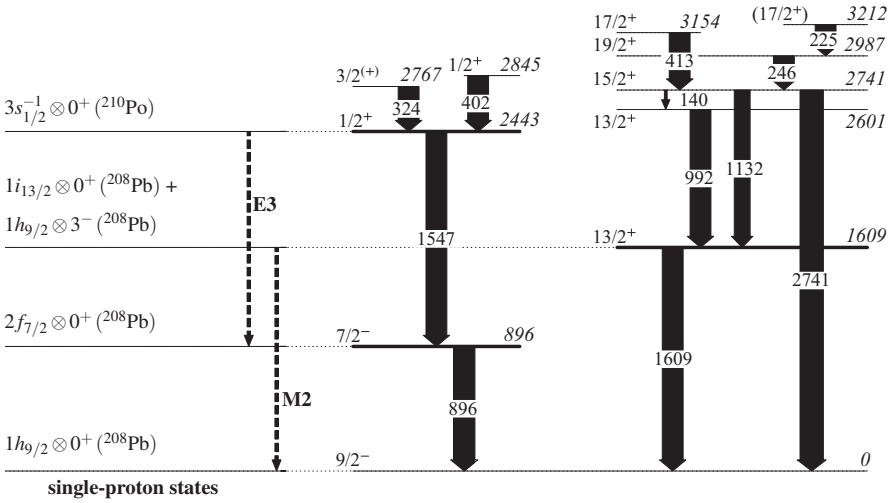

FIG. 1. The partial level scheme of the low-lying states in $^{209}_{83}$Bi. The dashed lines represent the pure multipole transitions, for which strengths are extracted in this work. The transition energies are given in keV and the width of the arrows represents the intensity of the transitions normalised to 100 % for the strongest transition from each level [21]. The thicker lines denote the levels for which decay spectra were analysed in this work.

respectively. It has also been independently measured to be 27(3)×10^3 e^{2}fm^6 [4] and 20(4)×10^3 e^{2}fm^6 [6] from inelastic scattering of $^{209}_{83}$Bi. Ref. [4] is in agreement with Ref. [8], but in disagreement with Ref. [7]. However, Ref. [6] is intermediate of Refs. [7, 8]. A study by Kratschmer et al. [22] found that the absolute transition rates between single-particle states and mixing ratios deduced from Ref. [7] may not be valid, as the bombarding energy of the α-beam was too high to produce pure Coulomb excitation. This casts doubts over the transition elements obtained, and thus no direct comparisons will be made between this result [7] and the result from this work. The $E3$ admixture in the wave-function of the 1609 keV transition depopulating this level, has been determined previously to be ∼10 % based on a measured mixing ratio of -0.33(10) [20]. Beene et al., combined this measured mixing ratio with a value of B($E3$;1609→0)=15(1)×10^3 e^{2}fm^6, quoted by Bohr and Mottelson [23], to derive a calculated value of T$_{\frac{1}{2}}$=0.29(15) ns [20] for the 1609 keV level. A weighted average using the results from Ref. [4] and Ref. [8], gives a B($E3\uparrow$)=26(3)×10^3 e^{2}fm^6 (equivalent to B($E3$;1609→0)=19(2)×10^3 e^{2}fm^6). Combining this value of the B($E3\downarrow$) with a measured mixing ratio of -0.33(10) [20] for the 1609 keV, yields a T$_{\frac{1}{2}}$=0.23(13) ns, similar to the calculated value in Ref. [20]. However, prior to this current work there has not been a direct measurement of the half-life.

The strength of the $3s_{\frac{1}{2}}\rightarrow 2f_{\frac{7}{2}}$ pure $E3$ transition can be obtained from the half-life of the first $\frac{1}{2}^+$ state at 2443 keV. This has been previously measured to be T$_{\frac{1}{2}}$=11.3(4) ns [3], and T$_{\frac{1}{2}}$=10(2) ns [24]. The $\frac{19}{2}^+$ level at 2987 keV is known to be isomeric with a half-life of 17.9(5) ns [3], but its lifetime could not be measured in this work.

II. EXPERIMENTAL SET-UP

Excited states in $^{209}_{83}$Bi were populated by bombarding an enriched (∼99 %), 20 mg·cm^{-2} $^{208}_{82}$Pb target with a 32-MeV ^{7}Li beam, delivered by the 9 MV tandem accelerator at the National Institute for Physics and Nuclear Engineering in Bucharest, Romania. The $^{208}_{82}$Pb(^{7}Li,2n$\alpha\gamma$)$^{209}_{83}$Bi, proton transfer reaction at around the barrier energy, was estimated to be ∼4 % of the total reaction cross-section [25]. Nuclei that were also produced in this experiment include: $^{210}_{83}$Bi [26, 27]; $^{212}_{84}$Po [28]; and $^{212,213}_{85}$At [28, 29], with the strongest side-channel being attributed to the 3n fusion-evaporation reaction ($^{212}_{85}$At).

The half-lives of the levels of interest were measured using γ-rays detected in *ROSPHERE* which is an ar-

ray of 14 Compton-suppressed HPGe detectors and 11 $LaBr_3$(Ce) scintillator detectors. The $LaBr_3$(Ce) and HPGe detectors were all placed ∼20 cm from the target position at forward and backward angles of 37°, 70° and 90° relative to the beam-axis. The 11 cylindrical $LaBr_3$(Ce) detectors in this setup comprised seven Ø2"×2" and four Ø1.5"×2" crystals, which were all 5% doped with Ce^{3+}. The data were recorded using either a HPGe-HPGe-HPGe or a HPGe-$LaBr_3$(Ce)-$LaBr_3$(Ce) triggering condition with a coincidence master gate time window of ∼50 ns. A total of $\sim 3.5\times10^7$ HPGe-$LaBr_3$(Ce)-$LaBr_3$(Ce) coincidences were recorded during the five-day experiment. The energy and efficiency calibrations for both the HPGe and $LaBr_3$(Ce) detectors were obtained using ^{152}Eu and ^{60}Co sources. The timing response of each detector was corrected offline for the low-energy time walk using a ^{152}Eu source, as described in Ref. [30].

For the angular distribution measurement, the 20 mg·cm^{-2} $^{208}_{82}$Pb target was orientated at 55° relative to the beam-axis. A co-axial detector, at a distance of 30 cm from the target position, was used to measure γ-ray intensities at 16 angles between -26.5° and +116.5°. A clover detector placed at 90° relative to the beam-axis acted as the monitor detector. Efficiencies at each of the measured angles were performed using both ^{60}Co and ^{152}Eu sources, placed at the target position. Lead shielding was placed in front of both the moving and monitor detector in an effort to reduce contamination lines from tantalum, which was present in both the beam stopper and collimator. Discs of copper, cadmium and aluminium were also placed around the front of both the moving and monitor HPGe detectors in order to reduce the detection of x-rays. The current of the ^{7}Li beam on the $^{208}_{82}$Pb target was roughly ∼8 pnA during the measurement at each angle.

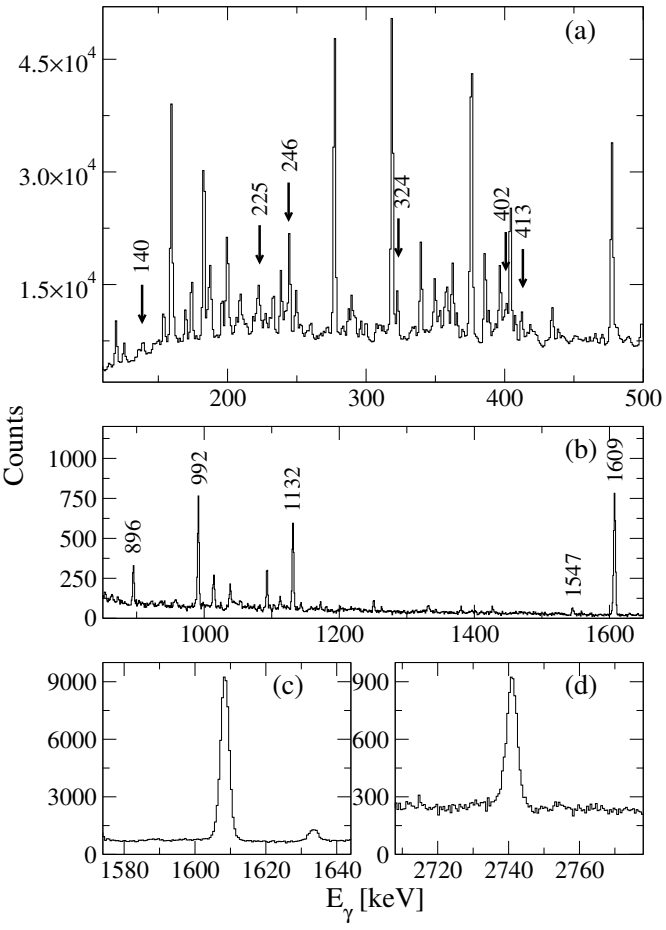

FIG. 2. The γ-ray energy spectra measured in the HPGe detectors: (a) The total projection of a (E_γ-E_γ) matrix, with the 140-, 225-, 246-, 324-, 402- and 413 keV $^{209}_{83}$Bi transitions used as gates marked by arrows. (b) An energy spectrum created as a result of using the gates in panel (a), with the high-energy γ-ray transitions of interest in $^{209}_{83}$Bi labelled with their energy. (c,d) show the cleanliness of the 1609- and 2741 keV transitions in the singles spectra, used for the angular distribution analysis.

III. DATA ANALYSIS AND RESULTS

The half-life data was collected and sorted offline into a series of γ-ray energy and time difference spectra, two-dimensional HPGe and $LaBr_3$(Ce) (E_γ-E_γ) matrices and three-dimensional E_{γ_1}-E_{γ_2}-ΔT cubes, and subsequently analysed using the GASPWARE and RADWARE packages [31, 32]. Fig. 2a shows a projection of the HPGe E_γ-E_γ matrix where the transitions used as gates in the HPGe detectors to select the cascades required in the $LaBr_3$(Ce) detectors to measure the $\frac{13}{2}^+_1$ and $\frac{7}{2}^-_1$ levels are denoted by the arrows. The cleanliness of this procedure can be seen in Fig. 2b where the transitions that were used to obtain the decay spectra are indicated. The corresponding $LaBr_3$(Ce) spectra are shown in Fig. 3, where (a) shows the result of applying gates on the **140-, 225-, 246-, and 413 keV transitions** in the HPGe detectors, and (b) the result of applying an additional gate on the 1609 keV transition in a $LaBr_3$(Ce) detector. The spectrum in Fig. 3b shows that it is possible to set clean gates in the $LaBr_3$(Ce) detectors on the 992- and 1132 keV transitions which feed the 1609 keV state.

Fig. 4a shows the forward and reverse time-difference spectra for the 896 keV level, obtained by gating on the photo-peaks of the feeding and de-exciting 1547- and 896 keV γ-ray transitions on the energy axes of an E_{γ_1}-E_{γ_2}-ΔT cube [30]. The cube was sorted with gates on the 324- and 402 keV transitions in the HPGe detectors. **The half-life of the $\frac{7}{2}^-_1$ level was previously calculated to be $T_{\frac{1}{2}}$=8.2(12) ps based on the B($E2\uparrow$) values from Refs. [1, 8, 22] and the adopted mixing ratio from Ref. [33].** This value of the half-life is consistent with the lack of a centroid shift between the two distributions in Fig. 4a and was used to determine a timing resolution of ∼350 ps at full-width half maximum (FWHM)

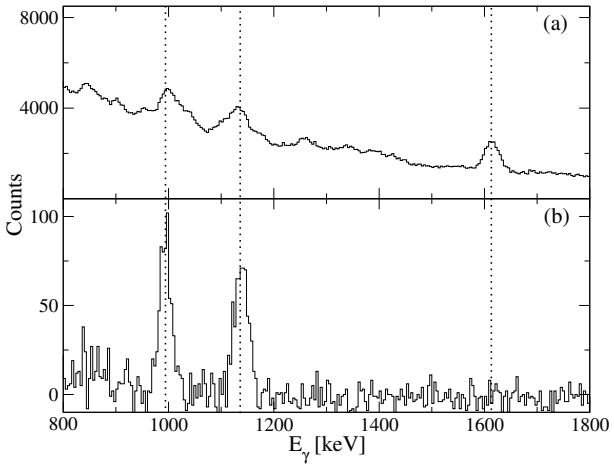

FIG. 3. The γ-ray energy spectra measured in the $LaBr_3$(Ce) detectors: (a) The total projection of the E_γ-E_γ matrix with gates in the HPGe detectors on the 140-, 225-, 246- and 413 keV transitions, and (b) with the addition of a gate on the 1609 keV transition in a $LaBr_3$(Ce) detector. The dashed lines indicate the positions of the feeding (992- and 1132 keV) and de-exciting (1609 keV) transitions for the $\frac{13}{2}^+_1$ state.

for the setup. The centroid shift measurement of the $\frac{13}{2}^+_1$ level uses gates on the photo-peaks of the $\frac{13}{2}^+_2 \rightarrow \frac{13}{2}^+_1$ (992 keV), $\frac{15}{2}^+_1 \rightarrow \frac{13}{2}^+_1$ (1132 keV) and $\frac{13}{2}^+_1 \rightarrow \frac{9}{2}^-$ (1609 keV) transitions shown in Figs. 3a and 3b. The timing distributions of the 992- and 1609 keV, and 1132- and 1609 keV coincidences were summed to give the forward and reverse time-difference spectra shown in Fig. 4b. The difference between these symmetric time distributions is twice the lifetime and gives a value of $T_{\frac{1}{2}}$=0.120(15) ns for the $\frac{13}{2}^+_1$ level. Fig 4c shows the individual points of the time curve for the same data, including the associated statistical uncertainty. This time curve was fitted with a convolution between the Prompt Response Function (PRF) shown in Fig. 4a and an exponential decay function. This method gives a value of $T_{\frac{1}{2}}$=0.130(10) ns, which is in good agreement with the value from the centroid shift method. However, this value has an uncertainty of only 10 ps, which is equivalent to the time resolution of the setup and is therefore thought to be underestimated. The accepted value of the half-life to be used in the subsequent discussions is therefore $T_{\frac{1}{2}}$=0.120(15) ns.

The forward time distribution of the $\frac{1}{2}^+_1$ isomeric state in Fig. 4d, was obtained by gating on the 896- and 1547 keV transitions in the HPGe detectors, and on the photo-peaks of the feeding (324- and 402 keV), and de-exciting (1547- and 896 keV, respectively) γ-ray transitions in the $LaBr_3$(Ce) detectors. Gating on the HPGe detectors allowed a very clean observation of the peaks of interest from the fast detectors due to the small number of coincident transitions (see Fig. 1). The

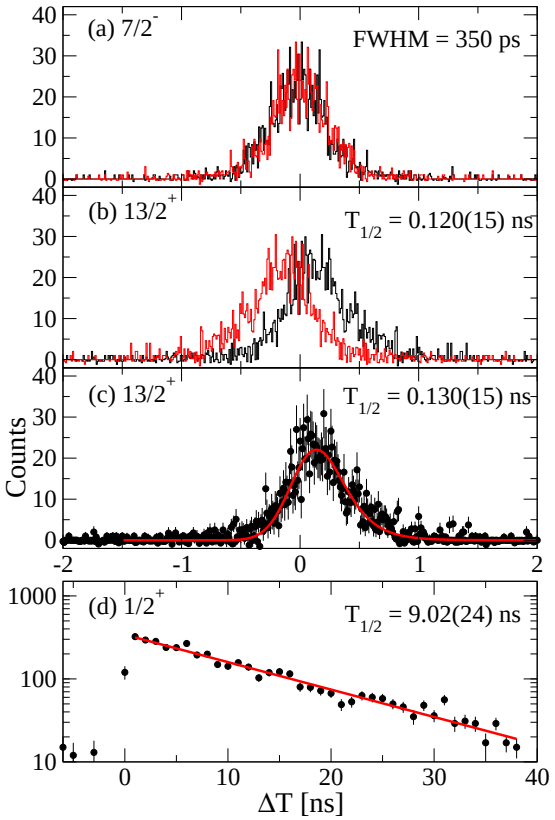

FIG. 4. (Colour Online) The forward (black) and reverse (red) time distributions for (a) the 896 keV state, obtained by gating on the 1547- and 896 keV coincidences and (b) the 1609 keV state, obtained by gating on the photo-peaks of the feeding (992- and 1132 keV) and de-exciting (1609 keV) transitions. The forward time profile of (c) the 1609 keV state using the same gates as in (b) and (d) the 2443 keV state, obtained by gating on the photo-peaks of the feeding (324- and 402 keV) and de-exciting (1547 keV) transitions.

resulting time distribution, shown in Fig. 1 with a 1 ns binning (much greater than the prompt time resolution of $\sim$ 350 ps (Fig. 4a) yields a value of $T_{\frac{1}{2}}$ = 9.02(24) ns. This value is within one standard deviation of the value reported by Ellegaard et al. [24], but differs significantly from the value of Demanins and Raicich [3] (within 3σ). Due to the lack of details on the data analysis in Ref. [3], the source of the discrepancy between these values is ambigious, but may be clarified in future studies.

In order to resolve the B($E3$) and B($M2$) contributions to the $1i_{\frac{13}{2}} \rightarrow 1h_{\frac{9}{2}}$ transition strength, the angular distribution of the 1609 keV transition was measured. Singles spectra as a function of angle were obtained for the 246-

, 1609- and 2741 keV transitions which de-populate the $\frac{19}{2}^+_1$, $\frac{13}{2}^+_1$ and $\frac{15}{2}^+_1$ levels respectively, as shown in Fig. 1. These transitions were the only transitions in $^{209}_{83}$Bi which were sufficiently clean or had enough statistics for an angular distribution measurement. The cleanliness of the 1609- and 2741 keV transitions in the HPGe singles spectrum is shown in Fig. 2c and Fig. 2d respectively. The measured γ-ray intensities as a function of angle, shown in Fig. 5, were interpreted using the expression [34]:

$$W(\theta) = A_0\big(1 + A_2B_2P_2(cos\theta) + A_4B_4P_4(cos\theta) + A_6B_6P_6(cos\theta)\big), \quad (1)$$

where A_0 is a normalising factor and the $A_{2,4,6}$ coefficients depend on the spins of the states involved in the transition and the mixing ratio of the γ-ray. The $B_{2,4,6}$ coefficients contain the alignment of the initial state, which was considered to be a Gaussian distribution centred about M=0 and parametrised as [35]:

$$w(M) = N \cdot exp[(-0.5M/\sigma)^2], \quad (2)$$

where N is a normalising factor such that $\Sigma\, w(M)$=1 and σ is a parameter in the fit. $P_{2,4,6}(\cos\theta)$ are the standard Legendre polynomial functions. The data were fitted using the STAG code which follows the method outlined in Ref. [35].

The 2741 keV transition decays from the $\frac{15}{2}^+_1$ level to the $\frac{9}{2}^-_1$ ground state and was used to evaluate the parameter σ, used in the alignment distribution described by Eq. 2 on the assumption that it is a stretched $E3$ transition. Fig. 5c shows the best fit to this data which was obtained with a value of σ=2.25, corresponding to $\frac{\sigma}{J}$=0.30. Using this as a starting point, the best fit for the 246 keV ($\frac{19}{2}^+ \rightarrow \frac{15}{2}^+$) transition (shown in Fig. 5a), was obtained for values of σ=2.24 ($\frac{\sigma}{J}$=0.24) and δ=0.02(2). The error on δ was obtained following the procedure outlined in Ref. [36]. The value of δ=0.02(2) is consistent with the expectation of a small $M3$ admixture in the ΔJ=2 transition. The best fit to the data for the 1609 keV transition between the $\frac{13}{2}^+_1 \rightarrow \frac{9}{2}^-$ states is shown in Fig. 5b. **The inset to Fig. 5b. shows the variation of χ^2 for the fit as a function of the mixing ratio of the transition, with the red line indicating a value of χ^2 which is 1.09 times the minimum. This is the multiplier calculated [36] for 13 degrees of freedom (16 data points 3 parameters in the fit A_0, δ, σ) and gives the value of chi-squared used to evaluate the error in delta. The best fit for this level was obtained for values of σ=2.14 ($\frac{\sigma}{J}$=0.33) and δ=-0.18(2). The value of δ which corresponds to σ=2.25 is δ=-0.20, is within the quoted error.**

The half-lives of the 1609- and 2443 keV states and the mixing ratio of the 1609 keV transition have been used in the following equations to derive the reduced transition probabilities [37]:

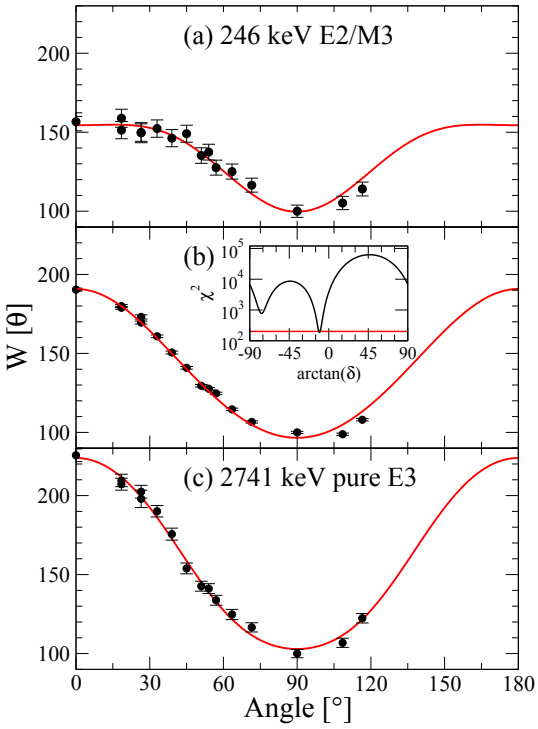

FIG. 5. (Colour Online) The γ-ray intensity as a function of angle for the (a) 246 mixed $E2/M3$ transition (b) 1609 keV transition and (c) 2741 keV pure $E3$ transition. The inset to (b) shows the χ^2 value as a function of arctan(δ).

$$B(M2) = \frac{5.12\times10^{-8}}{T_{\frac{1}{2}}E_\gamma^5}\frac{1}{(1+\delta^2_{\frac{E3}{M2}})}\mu_N^2 fm^2 \quad (3)$$

and

$$B(E3) = \frac{1.21\times10^{-3}}{T_{\frac{1}{2}}E_\gamma^7}\frac{\delta^2_{\frac{E3}{M2}}}{(1+\delta^2_{\frac{E3}{M2}})}e^2 fm^6, \quad (4)$$

where E_γ is the γ-ray energy in MeV and $T_{\frac{1}{2}}$ is the half-life of the state in seconds. The B(Lλ) values obtained using these equations are listed in Table I.

Both B($E3$) values of the 1609 keV transition from Refs. [4, 7], are independently consistent with the value from Hertel et al. [8]. Therefore, a weighted average of the B($E3\uparrow$) from Refs. [4, 6–8] was calculated. These transition probabilites were adjusted individually, so that the measured $E3$ excitation probability for the $1h_{\frac{9}{2}}(3^-)$ septuplet agreed with the assumed value of 7×10^5 e^{2}fm^6 for the 3$^-$ vibrational state in $^{208}_{82}$Pb [40]. This is the method proposed in Bohr and Mottelson [23] and yields B($E3\uparrow$)=24(4)×10^3 e^{2}fm^6, which is equivalent to B($E3\downarrow$)=17(3)×10^3 e^{2}fm^6.

TABLE I. Half-lives, measured and calculated B(Lλ) transition rates in ^{209}Bi.

E_x (keV)	J_i^π	$T_{\frac{1}{2}}$ (ns)	E_γ (keV)	J_f^π	Lλ	Measured Transitions	B(Lλ) ($\times10^3$) e^{2}fm^6 or μ_N^2fm^2	SM ($\times10^3$) e^{2}fm^6 or μ_N^2fm^2	FFS ($\times10^3$) e^{2}fm^6 or μ_N^2fm^2
1609	$\frac{13}{2}^+_1$	0.120(15)	1609	$\frac{9}{2}^-_1$	$E3$	(^{208}Pb $3^-\otimes\pi1h_{9/2}$)→(^{208}Pb $0^+\otimes\pi1h_{9/2}$)	13(2)	0.52	9.8 [38]
					$M2$	(^{208}Pb $0^+\otimes\pi1i_{13/2}$)→(^{208}Pb $0^+\otimes\pi1h_{9/2}$)	0.038(5)	0.43	0.033 [39]
2443	$\frac{1}{2}^+_1$	9.02(24)	1547	$\frac{7}{2}^-_1$	$E3$	(^{210}Po $0^+\otimes\pi3s_{1/2}$)→(^{208}Pb $0^+\otimes\pi2f_{7/2}$)	6.3(2)	0	-

This is in good agreement with the value of the B($E3$,$\frac{13}{2}^+_1\rightarrow\frac{9}{2}^-$) = 13(2)$\times10^3$ e^{2}fm^6 that has been determined from the measured half-life and mixing ratio in this work.

IV. DISCUSSION

Shell-model calculations in which the lowest $\frac{13}{2}^+_1$ and $\frac{9}{2}^-$ states are described as pure $\pi1i_{\frac{13}{2}}$ and $\pi1h_{\frac{9}{2}}$ configurations and the radial wave functions are obtained with the Skx Skyrme mean-field approximation [41], yield B($E3$,$\frac{13}{2}^+_1\rightarrow\frac{9}{2}^-$)=0.52$\times10^3$ e^{2}fm^6 and B($M2$,$\frac{13}{2}^+_1\rightarrow\frac{9}{2}^-$)=0.43$\times10^3$ μ_N^2fm^2 with free-nucleon charges and g-factors. These values are at least an order of magnitude different from the experimental values shown in Table I with the calculated B($E3$) value being too small and the calculated B($M2$) being too large. Calculations within the theory of Finite Fermi Systems (FFS), which takes into account the residual interaction between quasi-particles, eliminating the need for effective charges [38] yield B($E3$,$\frac{13}{2}^+\rightarrow\frac{9}{2}^-$)=9.8$\times10^3$ e^{2}fm^6. This value was calculated by adjusting the parameters of the effective particle-hole interactions. Calculations with an effective magnetic operator give B($M2$,$\frac{13}{2}^+_1\rightarrow\frac{9}{2}^-$)=33 $\mu_N^2 fm^2$ [39]. Both of these values are in good agreement with the measured ones.

The $\frac{1}{2}^+_1$ state at 2443 keV was observed to have a large spectroscopic factor in the ^{210}Po(t,α) [42] reaction and is therefore dominated by the excitation of a proton across the Z=82 shell gap to form a [($\pi\mathbf{1h}_{\frac{9}{2}}$)$^2_{0^+}\otimes$($\pi\mathbf{3s}_{\frac{1}{2}}{}^{-1}$)] configuration. The B($E3$) strength from this configuration to the $\pi\mathbf{2f}_{\frac{7}{2}}$ state at 896 keV is identically zero. Ellegaard et al. [24] suggest that the transition proceeds through an admixture of [($\pi\mathbf{2f}_{\frac{7}{2}}$)$^2_{0^+}\otimes$($\pi\mathbf{3s}_{\frac{1}{2}}{}^{-1}$)] in the wavefunction of the E_x=2443 keV $\frac{1}{2}^+_1$ state. The shell model calculations allowing the admixture of all the 1p-1h states considered in Ref. [43], gives a B($E3$,[($\pi\mathbf{2f}_{\frac{7}{2}}$)$^2_{0^+}\otimes$($\pi\mathbf{3s}_{\frac{1}{2}}{}^{-1}$)]→[$\pi\mathbf{2f}_{\frac{7}{2}}$)])=95$\times10^3$ e^{2}fm^6. A 6% admixture of this wavefunction into the pure configuration involving the $\pi\mathbf{1h}_{\frac{9}{2}}$ is required to explain the experimental value, in agreement with the result obtained by Ellegaard et al. [24].

V. SUMMARY

The results of the measurement of the half-life of the $\frac{13}{2}^+_1$ level ($T_{\frac{1}{2}}$=0.120(15) ns) and the $E3/M2$ mixing ratio for the 1609 keV transition (δ=-0.18(2)) have been combined to give B($E3$,$\frac{13}{2}^+_1\rightarrow\frac{9}{2}^-$)=13(2)$\times10^3$ e^{2}fm^6 and B($M2$,$\frac{13}{2}^+_1\rightarrow\frac{9}{2}^-$)=0.038(5)$\times10^3$ μ_N^2fm^2, corresponding to 4.4(7) and 0.7(1) W.u respectively. The results of calculations performed within the single-particle shell model are unable to reproduce these values but better agreement is obtained with calculations within the finite Fermi system [38, 39].

The half-life of the long-lived $\frac{1}{2}^+_1$ state at 2443 keV was measured to be 9.02(24) ns, which corresponds to B($E3$,$\frac{1}{2}^+_1\rightarrow\frac{7}{2}^-$)=6.3(2)$\times10^3$ e^{2}fm^6 (2.2(1) W.u.). This transition is strictly forbidden in the single-particle shell-model but can be explained by a small (∼6%) admixture in the wavefunction of the $\frac{1}{2}^+_1$ state [24].

ACKNOWLEDGMENTS

The staff of the Horia Hulubei National Institute of Physics and Nuclear Engineering (IFIN-HH), Bucharest, Romania are thanked for their excellent technical support during this experiment. This work was supported by the UK NuSTAR grant (ST/G000697/1) from the Science and Technology Facilities Council (STFC) and NSF grant PHY-1404442. OJR acknowledges support from Science Foundation Ireland under Grant No. 12/IP/1288. TA acknowledges support from Almajmaah University, Saudi Arabia. The work of N. M. Florea has been funded by the Sectoral Operational Programme Human Resources Development 2007-2013 of the Ministry of European Funds through the Financial Agreement POSDRU/159/1.5/S/132397.

[1] O. Häusser, F.C. Khanna and D. Ward, Nuclear Physics A **194**, 113 (1972).

[2] J.F. Ziegler and G.A. Peterson, Physical Review **165**,

1337 (1968).
[3] F. Demanins and F. Raicich, Il Nuovo Cimento **109 A**, 5 (1996).
[4] A. Scott, M. Owais, and F. Petrovich, Nuclear Physics **A 226**, 109 (1974).
[5] W. Benenson, S.M. Austin, P.J. Locard, F. Petrovich, J.R. Borysowicz and H. McManus , Physical Review Letters **24**, 907 (1970).
[6] J.Ungrun, R.M. Diamond, P.O. Tjøm and B.Elbek , Mat. Fys. Medd. Dan. Vid. Selsk. **38**, 8 (1971).
[7] R.A. Broglia, J.S. Lilley, R. Perazzo and W.R. Phillips, Physical Review C **1**, 1508 (1970).
[8] J.W. Hertel, D.G. Fleming, J.P. Schiffer and H.E. Gove, Physical Review Letters **23**, 488 (1969).
[9] E. Grosse, M. Dost, K. Haberkant, J.W. Hertel, H.V. Klapdor, H.J. Körner, D. Proetel and P. Von Brentano, Nuclear Physics A **174**, 525 (1971).
[10] O. Nathan, Nuclear Physics **30**, 332 (1962).
[11] D.S. Andreev, J.Z. Gangrskij, C. Lemberg and V.A. Nabinoritschvili, Izv. Akad. Nauk. SSSR **29**, 2231 (1965).
[12] P. Salling, Physics Letters **17**, 139 (1965).
[13] H.J. Körner, K. Auerbach, J. Braunsfurth and E. Gerdau, Nuclear Physics **86**, 395 (1966).
[14] J.L. Quebert, K. Nakai, R.M. Diamond and F.S. Stephens, Nuclear Physics **A 150**, 68 (1970).
[15] O. Häusser, A.B. McDonald, T.K. Alexander, A.J. Ferguson and R.E. Warner, Physics Letters B **38**, 75 (1972).
[16] G. Astner, I. Bergström, J. Blomqvist, B. Fant and K. Wikström, Nuclear Physics A **182**, 219 (1972).
[17] A. Bohr and B.R. Mottelson, Nuclear Structure, Vol I: Nuclear Deformations, World Scientific Publishing Co., Chapter 3 (1969).
[18] B.R. Mottelson, Nikko Summer School Lectures 1967, NORDITA publication No.288, (1967).
[19] K. Arita and H. Horie, Physics Letters B **30**, 14 (1969).
[20] J.R. Beene, O. Häusser, T.K. Alexander and A.B. McDonald, Physical Review C **17**, 1359 (1978).
[21] K.H. Maier, T. Nail, R.K. Sheline, W. Stöffl, J.A. Becker, J.B. Carlson, R.G. Lanier, L.G. Mann, G.L. Struble, J.A. Cizewski and B.H. Erkkila, Physical Review C **27**, 1431 (1983).
[22] W. Kratschmer, H.V. Klapdor and E. Grosse, Nuclear Physics A **201**, 179 (1973).
[23] A. Bohr and B.R. Mottelson, Nuclear Structure, Vol II: Nuclear Deformations, World Scientific Publishing Co., Chapter 6, 565 (1998).
[24] C. Ellegaard, R. Julin, J. Kantele, M. Luontama and T. Poikolainen, Nuclear Physics A **302**, 125 (1978).
[25] O.B. Tarasov and D. Bazin, Nuclear Instruments and Methods in Physics Research B **204**, 174 (2003).
[26] H.T. Motz, E.T. Jurney, E.B. Shera and R.K. Sheline, Physical Review Letters **26**, 854 (1971).
[27] R.K. Sheline, R.L. Ponting, A.K. Jain, J. Kvasil, B. du Nianga and L. Nkwambiaya, Czech. J. Phys. B **39**, 22 (1989).
[28] T.P. Sjoreen, U. Garg and D.B. Fossan, Physical Review C, **21**, 1838 (1980).
[29] S. Bayer, A.P. Byrne, G.D. Dracoulis, A.M. Baxter, T. Kibédi, F.G. Kondev, S.M. Mullins and T.R. McGoram, Nuclear Physics A, **650**, 3 (1999).
[30] N. Mărginean, D.L. Balabanski, D. Bucurescu, S. Lalkovski, L. Atanasova, G. Căta-Danil, I. Căta-Danil, J.M. Daugas, D. Deleanu, P. Detistov, G. Deyanova, D. Filipescu, G. Georgiev, D. Ghiţă, K.A. Gladnishki, R. Lozeva, T. Glodariu, M. Ivaşcu, S. Kisyov, C. Mihai, R. Mărginean, A. Negret, S. Pascu, D. Radulov, T. Sava, L. Stroe, G. Suliman and N.V. Zamfir, European Physical Journal A **46**, 329 (2010).
[31] D. Bazzacco and N. Mărginean, (private communication).
[32] D. Radford, Nuclear Instruments and Methods in Physics Research A **361**, 297 (1995).
[33] G.R. Hagee, R.C. Lange and J.T. McCarthy, Nuclear Physics **84**, 62 (1966).
[34] H. Frauenfelder and R.M. Steffen, 'Angular distribution of nuclear radiation' in α, β and γ-ray spectroscopy, ed. K Siegbahn, North Holland (1965).
[35] P.A. Butler and P.J. Nolan, Nuclear Instruments and Methods **190**, 283 (1981).
[36] A.N. James and P.J. Twin and P.A. Butler, Nuclear Instruments and Methods **115**, 105 (1974).
[37] K. Alder and R.M. Steffen, Chapter 2: The Emission of Gamma Radiation and Nuclear Structure, The Electromagnetic Interaction in Nuclear Spectroscopy, North Holland, pp. 39 (1975).
[38] P. Ring, R. Bauer and J. Speth, Nuclear Physics A **206**, 97 (1973).
[39] R. Bauer, J. Speth, V. Klemt, P. Ring, E. Werner and T. Yamazaki, Nuclear Physics A **209**, 35 (1973).
[40] A. Bohr and B.R. Mottelson, Nuclear Structure, Vol II: Nuclear Deformations, World Scientific Publishing Co., Chapter 6, pp. 561 (1998)
[41] B.A. Brown, Physical Review C **58**, 220 (1998).
[42] P.D. Barnes, E. Romberg, C. Ellegaard, R.F. Casten, O. Hansen, T.J. Mulligan, R.A. Broglia and R. Liotta, Nuclear Physics A **195**, 146 (1972).
[43] B.A. Brown, Physical Review Letters **85**, 5300 (2000).